Journal of Photochemistry and Photobiology B: Biology xxx (2014) xxx–xxx

Contents lists available at ScienceDirect

Journal of Photochemistry and Photobiology B: Biology

journal homepage: www.elsevier.com/locate/jphotobiol

Photocatalytic H_2 evolution from NADH with carbon quantum dots/Pt and 2-phenyl-4-(1-naphthyl)quinolinium ion

Wenting Wu [a], Liying Zhan [a], Kei Ohkubo [b], Yusuke Yamada [b], Mingbo Wu [a], Shunichi Fukuzumi [b,*]

[a] State Key Laboratory of Heavy Oil Processing, School of Chemical Engineering, China University of Petroleum, Qingdao 266555, PR China
[b] Department of Material and Life Science, Graduate School of Engineering, Osaka University, ALCA, Japan Science and Technology Agency (JST), Suita, Osaka 565-0871, Japan

ARTICLE INFO

Article history:
Received 3 October 2014
Received in revised form 28 October 2014
Accepted 30 October 2014
Available online xxxx

ABSTRACT

Carbon quantum dots (CQDs) were simply blended with platinum salts (K_2PtCl_4 and K_2PtCl_6) and converted into a hydrogen-evolution co-catalyst *in situ*, wherein Pt salts were dispersed on the surface of CQDs under photoirradiation of an aqueous solution of NADH (an electron and proton source) and 2-phenyl-4-(1-naphthyl)quinolinium ion ($QuPh^+$–NA) employed as an organic photocatalyst. The co-catalyst (CQDs/Pt) exhibits similar catalytic reactivity in H_2 evolution as that of pure Pt nanoparticles (PtNPs) although the Pt amount of CQDs/Pt was only 1/200 that of PtNPs previously reported. CQDs were able to capture the Pt salt acting as Pt supports. Meanwhile, CQDs act as electron reservoir, playing an important role to enhance electron transfer from $QuPh^+$–NA to the Pt salt, which was confirmed by kinetic studies, XPS and HRTEM.

1. Introduction

Hydrogen (H_2) is regarded as a clean fuel of the next generation because of its high energy density per weight, environmentally benign properties of nonemission of greenhouse gas and other harmful chemicals after burning [1–14]. Typically, a photocatalytic H_2-evolution system, which is an essential part of artificial photosynthesis, is composed of a sacrificial electron donor, a photocatalyst with long-lived charge-separated state upon photoexcitation and an H_2-evolution catalyst [8,15–19]. Up to date, one of the most efficient catalyst used for H_2 evolution is Pt nanoparticles (PtNPs), because Pt has a low over potential for proton reduction to evolve hydrogen [19,20]. However, due to the scarcity and high cost, the wide use of PtNPs is impeditive. Consequently, it is highly desired to reduce the amount of Pt in the catalytic system. A great deal of efforts have been devoted to prepare PtNPs as small as possible to reduce the amount of Pt. PtNPs with size of a few nanometers have been successfully synthesized on a supporting material such as Pt/C [21–31]. Their catalytic activities are greatly influenced by the particle size, surface structure, and the metal/support interfaces [32–37]. At the same time, PtNPs loaded on special position of support were prepared to reduce the amount of Pt and to improve the photocatalytic activities [38,39]. Recently, a new way to form H_2-evolution catalysts from metal salts inside the mesopores of silica–alumina loading photosensitizers with long-lived electron-transfer (ET) state has been developed, wherein the metal salts were reduced *in situ* in the reaction solution to form smaller size metal nanoparticles [40]. Although the lifetime of the ET state could be prolonged by supporting donor–acceptor linked dyads on mesoporous silica–alumina, the H_2 yield still needs to be improved. To some extent, it may be due to the poor electron-transfer ability of mesoporous silica–alumina itself, which prohibits the electron transfer between the photocatalyst and H_2-evolution catalysts [40].

Fortunately, carbon quantum dots (CQDs), as a rising star in nanocarbon family, may be a good candidate to serve as a support because of their unique electron-reservoir ability, efficient electron transfer, excellent water dispersibility, chemical stability, nano size, abundant/inexpensive nature and nontoxicity [41–44]. Owing to these advantages, CQDs have previously decorated PtNPs to improve their photocatalytic H_2 production [45–47]. The process of PtNPs' preparation is also difficult to be controlled, causing a loss of Pt.

Herein, in order to reduce Pt content and to make good use of Pt in the photocatalytic H_2 production, CQDs/Pt co-catalyst were *in-situ* prepared from CQDs and little amount of Pt salts (K_2PtCl_4 and K_2PtCl_6). Pt species can be deposited on CQDs to form CQDs/Pt co-catalyst. The H_2 evolution activity with CQDs/Pt co-catalyst was examined in the system composed of 2-phenyl-4-(1-naphthyl)quinolinium ion ($QuPh^+$–NA: photocatalyst) and dihydronicotinamide adenine dinucleotide (NADH: electron donor). The whole reaction scheme is depicted in Scheme 1. Kinetic studies, high-resolution transmission electron microscopy (HRTEM) images

* Corresponding author. Tel.: +81 6 6879 7368.
E-mail address: fukuzumi@chem.eng.osaka-u.ac.jp (S. Fukuzumi).

http://dx.doi.org/10.1016/j.jphotobiol.2014.10.018
1011-1344/

and X-ray photoelectron spectroscopy (XPS) were used to confirm that CQDs as electron reservoir play an important role to enhance electron transfer from the organic photocatalyst ($QuPh^{\cdot}-NA$) to Pt salts.

2. Materials and methods

2.1. Materials

EDTA-2Na·2H_2O, K_2PtCl_4 and K_2PtCl_6 were purchased from Sigma–Aldrich. 2-Phenyl-4-(1-naphtyl)quinolinium perchlorate ($QuPh^{+}-NA$) was synthesized by the reported method [48]. Each buffer solution was prepared by addition of NaOH to an aqueous solution containing 50 mM of electrolyte (phthalate for pH 4.5, phosphate for pH 7.0 or 8.0, or boric acid /potassium chloride for pH 9.0) or 25 mM of carbonate for pH 10. All chemicals were used without further purification.

2.2. Preparation of CQDs from EDTA-2Na

EDTA-2Na·2H_2O containing relatively stable carboxylate anions (COO^{-}) was chosen as the precursor. After pyrolysis under low temperature, COO^{-} can remain and thus render the CQDs soluble in water, and easily capture Pt cation. EDTA-2Na·2H_2O (1.6 g) was calcined in a tube furnace at 350 °C for 2 h at a heating rate of 5 °C min^{-1} in a N_2 atmosphere. The product was ground and dispersed in water (100 mL), and then centrifuged at a high speed (10,000 rpm) for 20 min. The upper brown dispersion was filtered with slow-speed quantitative microporous filter paper (0.25 μm) to remove the non-fluorescent deposit. The filtrate was dialyzed with MD34 (3500 Da) dialysis tube for 48 h to remove the remaining salts and small fragments. Pure luminescent CQDs powder was obtained by drying the concentrated solution at 60 °C for 24 h.

2.3. Characterization of CQDs

High-resolution transmission electron microscopy (HRTEM) images were taken on a JEOL JEM-2100UHR microscope with an accelerating voltage of 200 kV. Further evidence for the composition of the product was inferred from X-ray photoelectron spectroscopy (XPS), using a Thermo Scientific ESCALAB 250Xi spectrometer equipped with a pre-reduction chamber. Fourier transform infrared (FT-IR) spectra were recorded on a Nicolet 6700 spectrometer. Raman spectroscopy was recorded using an Ar^{+} ion laser at 514.5 nm (Renishaw in via 2000 Raman microscope, Renishaw plc, UK) to assess the graphitic structure of raw materials and products.

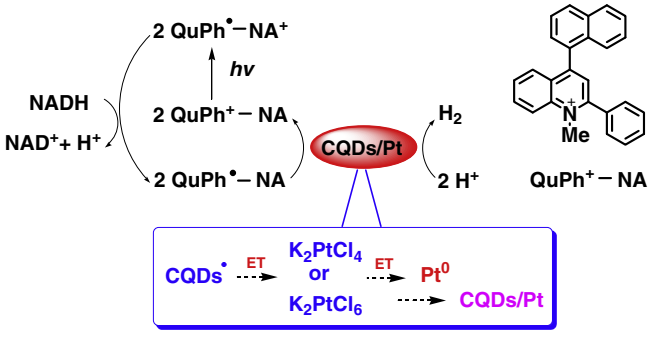

Scheme 1. Structure of $QuPh^{+}-NA$ and the overall catalytic cycle for photocatalytic hydrogen evolution.

2.4. Photocatalytic hydrogen evolution

A mixed solution (2.0 mL) of an aqueous buffer (pH 4.5, 7.0, 8.0, 9.0 or 10) and MeCN [1:1 (v/v)] containing $QuPh^{+}$–NA (0.22 mM), NADH (1.0 mM), CQDs, K_2PtCl_4 or K_2PtCl_6 was flushed with N_2 gas. The solution was then irradiated with a Xe lamp (Ushio Optical, Model X SX-UID 500X AMQ) through a color filter glass (Toshiba Glass UV-35) transmitting $\lambda > 340$ nm at room temperature. The gas in the headspace was analyzed using a Shimadzu GC-14B gas chromatograph (detector, TCD; column temperature, 50 °C; column, active carbon with 60–80 mesh particle size; carrier gas, N_2) to quantify the evolved hydrogen.

2.5. Kinetic measurements

A mixed solution (2.0 mL) of a deaerated aqueous buffer (pH 7.0) and MeCN [1:1 (v/v)] containing $QuPh^{+}$–NA (0.44 mM) and NADH (1.0 mM) was photoirradiated for 15 min with a Xe lamp through a color filter glass transmitting $\lambda > 340$ nm. Next, a deaerated aqueous solution containing CQDs, K_2PtCl_4, K_2PtCl_6, CQD/K_2PtCl_4 or CQDs/K_2PtCl_6 was added to the photoirradiated solution using a microsyringe with stirring. Rate constants of electron transfer from $QuPh^{\cdot}$–NA (obtained by one-electron reduction of $QuPh^{+}$–NA) to the catalyst were determined from the decay of absorption at 510 nm due to $QuPh^{\cdot}$–NA, which was monitored using a Hewlett–Packard 8453 diode array spectrophotometer with a quartz cuvette (path length 10 mm) at 298 K.

3. Results and discussion

3.1. Characterization of CQDs

The uniformity of the as-synthesized CQDs is clearly shown in Fig. 1. The diameters of CQDs are centered at 2–3 nm from transmission electron microscopy (TEM) images. High-resolution TEM (HRTEM) images of CQDs show well-resolved lattice fringes with interplanar spacings of 0.20 nm, which are close to the (100) diffraction facets of graphite carbon. The Raman peaks centered at ~1334 and 1561 cm^{-1} for the CQDs are attributed to the D and G bands of carbon materials representing the sp^3 and sp^2 carbon, respectively (see Supporting Information Fig. S1). The intensity ratio of the D and G bands (I_D/I_G) is a measure of the disorder extent, as well as the ratio of sp^3/sp^2 carbons. The I_D/I_G ratio of CQDs is 0.7775, indicating that sp^2 hybridization C was much more than sp^3 hybridization C [49]. Therefore, the above results suggest that CQDs are composed of nanocrystalline cores of graphitic sp^2 carbon atoms, and it will benefit for the electron reservoir and efficient electron transfer [44].

The chemical compositions and structures of the CQDs were further investigated. X-ray photoelectron spectroscopy (XPS) measurements show that carbon (C1s, 283 eV), nitrogen (N1s, 398 eV), and oxygen (O1s, 530 eV) elements were contained in CQDs. The XPS spectrum of C1s from CQDs can be deconvoluted into three smaller peaks, which are ascribed to the following functional groups: sp^3 bonded carbon (C—C, 283.0 eV), sp^2 bonded carbon (C=C, 283.8 eV) and epoxy/hydroxyls (C—O, 286.4 eV) (Fig. 2) [50,51]. The O1s spectrum could be deconvoluted into three peaks of C=O (529.4 eV), C—O (530.3 eV) and chemisorbed oxygen (COOH) and/or bound water (533.6 eV) [52,53]. Elemental analysis also confirmed the composition of CQDs (C: 42.01%, H: 5.83%, N: 9.95%). In the fourier transform infrared spectroscopy (FT-IR) analysis of CQDs (see Supporting Information Fig. S2), the absorption bands from 1113 to 1263 cm^{-1} are assigned to a C—O—C stretching and deformation vibrations, and those at 716, 851 and 1600 cm^{-1} are characteristic of benzene ring. The residue peaks at 1329 cm^{-1}

Please cite this article in press as: W. Wu et al., Photocatalytic H_2 evolution from NADH with carbon quantum dots/Pt and 2-phenyl-4-(1-naphthyl)quinolinium ion, J. Photochem. Photobiol. B: Biol. (2014), http://dx.doi.org/10.1016/j.jphotobiol.2014.10.018

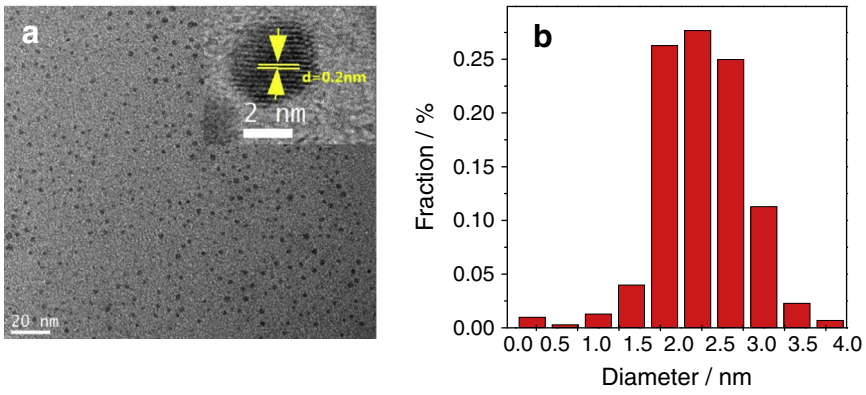

Fig. 1. (a) TEM image of CQDs and (b) the corresponding distribution.

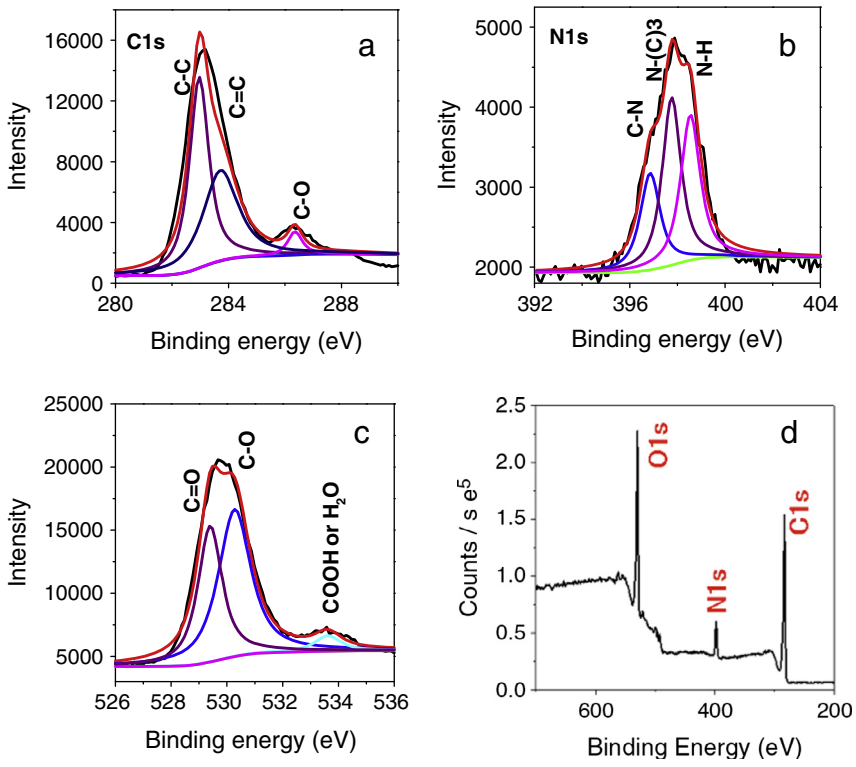

Fig. 2. High-resolution XPS spectra of CQDS (a) C1s, (b) O1s, (c) N1s and (d) XPS survey spectra.

and 998 cm^{-1} are assigned to O—C=O and C—OH stretching vibrations, respectively. Therefore, CQDs are graphite nanoparticles with oxygen-containing functional groups, which not only improve the water solubility but also provide "hands" to capture Pt salts via electrostatic force and van der Waals force.

3.2. Photocatalytic H_2 evolution of ratio-controlled CQDs with Pt salts (K_2PtCl_4 and K_2PtCl_6)

CQDs and Pt salts (K_2PtCl_4 and K_2PtCl_6) used as hydrogen-evolution co-catalysts were prepared by simple mixture. Fig. 3 shows the time courses of H_2 evolution under photoirradiation ($\lambda > 340$ nm) of a mixed solution (2.0 mL) of KH_2PO_4 buffers (pH 7.0) and MeCN [1:1 (v/v)] containing $QuPh^+$–NA (0.22 mM), NADH (1.0 mM), various ratio of CQDs and Pt salts. $QuPh^+$–NA efficiently absorbs the light at wavelengths longer than 340 nm as reported previously, and NADH was used as a sacrificial electron donor, which can afford the stoichiometric amount of H_2 (2.0 μmol) [54]. Without $QuPh^+$–NA, CQDs or Pt salts, no hydrogen evolution was observed from the mixed solution under the same reaction conditions. H_2 evolution with various ratios of CQDs and Pt salts were optimized as follows. When the weight ratio of CQDs/ K_2PtCl_6 comes to 5:4 (CQDs: Pt = 15:4), the H_2-evolution rate is higher than other ratios. The H_2 yield with co-catalyst (CQDs: K_2PtCl_6 = 5:4) could come to 95%, which is calculated from the amount of NADH used in the reaction, wherein the stoichiometric amount (2.0 μmol) of H_2 was produced in the reaction with PtNPs under the same conditions. For co-catalyst of CQDs/K_2PtCl_4, the optimization ratio of CQDs and K_2PtCl_4 was 3:2 (CQDs: Pt = 15:4). After irradiation the mixed solution with CQDs/K_2PtCl_4 co-catalyst for 40 min, the amount of evolved H_2 reached 1.6 μmol (80% yield) which is higher than that of CQDs/K_2PtCl_6 co-catalyst (1.35 μmol).

Please cite this article in press as: W. Wu et al., Photocatalytic H_2 evolution from NADH with carbon quantum dots/Pt and 2-phenyl-4-(1-naphthyl)quinolinium ion, J. Photochem. Photobiol. B: Biol. (2014), http://dx.doi.org/10.1016/j.jphotobiol.2014.10.018

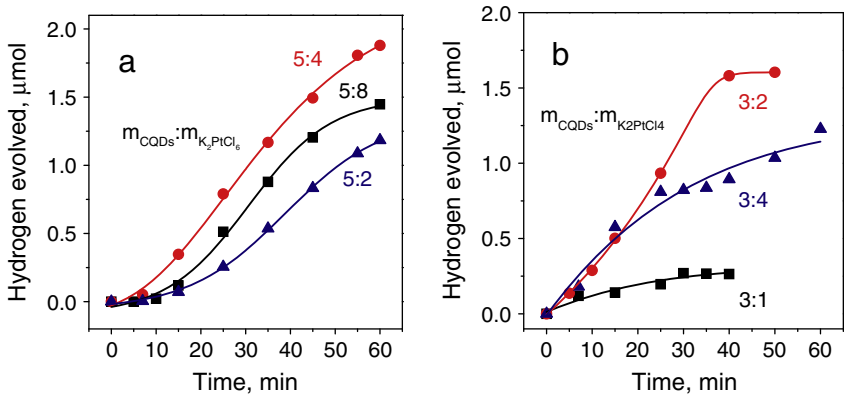

Fig. 3. Time courses of hydrogen evolution under photoirradiation ($\lambda > 340$ nm) of deaerated mixed solutions (2 mL) of KH_2PO_4 buffers (pH = 7.0) and MeCN [1:1 (v/v)] containing $QuPh^+$–NA (0.22 mM), NADH (1.0 mM), various loadings of CQDs (4.7 mg L^{-1}, 9.4 mg L^{-1} and 18.8 mg L^{-1}) and (a) K_2PtCl_6 (7.29 mg L^{-1} 15 μmol L^{-1}). When the weight ratio of CQDs and K_2PtCl_4 is 5:4, the mixed solution gives the best performance. (b) K_2PtCl_4 (6.23 mg L^{-1}, 15 μM). When the weight ratio of CQDs and K_2PtCl_4 is 3:2 (K_2PtCl_4 = 6.23 mg L^{-1}, 15 μM, CQDs = 9.4 mg L^{-1}), the mixed solution gives the best performance.

3.3. Photocatalytic H_2 evolution with CQDs/Pt salts under various pH conditions

The photocatalytic H_2-evolution experiments were performed with a mixture of an aqueous buffer and MeCN [1:1 (v/v)] containing $QuPh^+$–NA (0.22 mM), NADH (1.0 mM), CQDs (9.4 mg L^{-1}) and K_2PtCl_6 (7.29 mg L^{-1}, 15 μM) or K_2PtCl_4 (6.23 mg L^{-1}, 15 μmol) under various pH conditions. Fig. 4 shows the amount of evolved H_2 as a function of photoirradiation time at pH 4.5, 7.0, 8.0, 9.0 and 10. For CQDs/K_2PtCl_4 co-catalyst, the amount of evolved H_2 at pH 7.0 reached 1.6 μmol (80% yield) after 40 min, which is about twice of that at pH 4.5 and 8.0. The catalytic reactivity of CQDs/K_2PtCl_6 co-catalyst for photocatalytic H_2 evolution was also examined under various pH conditions. Fig. 4b shows the time course of photocatalytic H_2 evolution using CQDs/K_2PtCl_6 as the hydrogen-evolution catalyst under the same reaction conditions as the case of CQDs/K_2PtCl_4. Compared with CQDs/K_2PtCl_4 co-catalyst, CQDs/K_2PtCl_6 co-catalyst shows more efficient H_2 evolution at pH 7.0 and 8.0, respectively. After irradiation of the mixed solution with CQDs/K_2PtCl_6 co-catalyst at pH 8.0 for 50 min, the amount of evolved H_2 was 1.4 μmol (70% yield). Unlike conventional H_2 evolution systems which exhibit better performance under acid conditions, the CQDs/Pt salt can act as good H_2 evolution catalyst under neutral or weakly alkaline conditions. Under such conditions, carboxylic acid moieties (—COOH) contained in CODs are converted into carboxylate anion ($—COO^-$), which can capture Pt cation easily on the surface of CQDs and synergistically catalyze the hydrogen evolution.

3.4. Repetitive photocatalytic H_2 evolution with CQDs/Pt salts

The robustness of the CQDs/Pt co-catalyst was scrutinized by the repeated use in the photocatalytic H_2 evolution. The photocatalytic H_2 evolution was repetitively performed by photoirradiation ($\lambda > 340$ nm) of a deaerated mixed solution (2.0 mL) of a KH_2PO_4 buffer (pH 7.0) and MeCN containing NADH (1.0 mM), $QuPh^+$–NA (0.22 mM), CQDs (9.4 mg L^{-1}) and Pt salts (15 μM). After each catalytic reaction, a concentrated solution of NADH was added to the solution (twice). Time courses of the H_2 evolution are shown in Fig. 5. In the case of the photocatalytic reaction with CQDs/K_2PtCl_6 for the first time, the total amount of evolved H_2 reached 1.8 μmol in 1 h. During this time, K_2PtCl_6 was reduced by CQDs to form Pt metal species that act as an actual H_2 evolution catalysts. After 1st cycle, a concentrated solution of NADH was added to the solution, the reuse of the CQDs/K_2PtCl_6 with photodeposited Pt species resulted in faster and more H_2 evolution (1.9 μmol) in 1 h, even in the 3rd cycle. The faster H_2-evolution resulted from the removal of K_2PtCl_6, which partly disturbs $QuPh^+$–NA from the photoexcitation (vide infra). Thus, Pt species deposited on the CQDs act as the efficient H_2-evolution catalyst. Similarly, faster H_2 evolution with CQDs/K_2PtCl_4 in the 2nd cycle compared with the 1st cycle was also observed when NADH

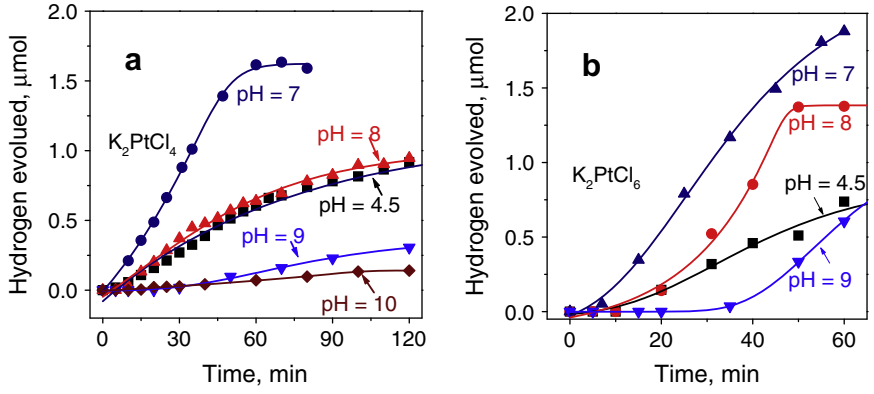

Fig. 4. Time courses of evolved hydrogen under photoirradiation ($\lambda > 340$ nm) of deaerated mixed solutions (2 mL) of aqueous buffers at various pH values and MeCN [1:1 (v/v)] containing $QuPh^+$–NA (0.22 mM), NADH (1.0 mM), CQDs (9.4 mg L^{-1}) (a) K_2PtCl_4 (6.23 mg L^{-1}, 15 μmol) with CQDs (9.4 mg L^{-1}); (b) K_2PtCl_6 (7.29 mg L^{-1}, 15 μM).

Please cite this article in press as: W. Wu et al., Photocatalytic H_2 evolution from NADH with carbon quantum dots/Pt and 2-phenyl-4-(1-naphthyl)quinolinium ion, J. Photochem. Photobiol. B: Biol. (2014), http://dx.doi.org/10.1016/j.jphotobiol.2014.10.018

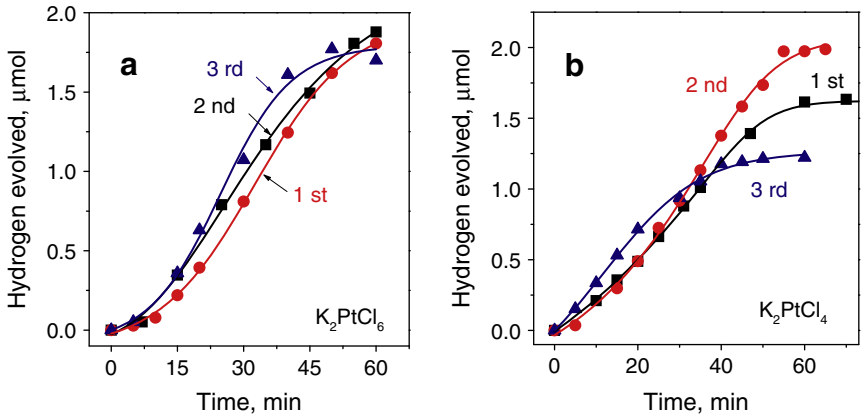

Fig. 5. Time courses of H_2 evolution in the repetitive photocatalytic reactions. H_2 evolution was examined by photoirradiation ($\lambda > 340$ nm) of a deaerated mixed solution (2.0 mL) of a KH_2PO_4 buffers (pH 7.0) and MeCN [1:1 (v/v)] containing $QuPh^+$–NA (0.22 mM), NADH (1.0 mM), CQDs (9.4 mg L^{-1}) and (a) K_2PtCl_6 (7.29 mg L^{-1}, 15 μM) or (b) K_2PtCl_4 (6.23 mg L^{-1}, 15 μmol). The mixed solution of a KH_2PO_4 buffers and MeCN [1:1 (v/v)] containing NADH was added to the reaction solution three times after each run.

(1.0 mM) was added as a sacrificial electron donor (Fig. 5b). At the 3rd cycle, the H_2 evolution rate at the initial 30 min was faster than that at the 1st and 2nd cycles. Unfortunately, the amount of evolved H_2 at the 3rd cycle could not reach as much as the amount at the 1st cycle.

3.5. H_2 evolution of CQDs/Pt salt under ultra-lower concentration

In order to reduce Pt content, the photocatalytic hydrogen evolution was performed by using low content of Pt salts and CQDs in a mixture of KH_2PO_4 buffer (pH 7.0) and MeCN [1:1 (v/v)] containing $QuPh^+$–NA (0.22 mM), NADH (1.0 mM), as shown in Fig. 6. When the original concentrations of K_2PtCl_6 and CQDs were reduced to 1/50, the H_2 evolution rate became even faster than that with the original concentration (Fig. 6a), because the low content of K_2PtCl_6 and CQDs resulted in more effective absorption of light by $QuPh^+$–NA alone with less absorption by CODS/Pt. Further reduction of the concentration of CQDs and K_2PtCl_6 to 1/100 of the original concentrations resulted in the slower H_2 evolution rate (Fig. 6a). In the case of CQDs/K_2PtCl_4 co-catalyst, however, the amount of evolved H_2 was 1/4 and 1/8 of that with original concentration when the concentrations of K_2PtCl_4 and CQDs were diluted to 1/50 and 1/100, respectively. Such a difference between K_2PtCl_6 and K_2PtCl_4 may result from the slower rate of electron transfer from $QuPh^·$–NA, which is produced by photoinduced electron transfer from NADH to QuPh–NA, to K_2PtCl_4 than that to K_2PtCl_6 (vide infra).

The amount of evolved H_2 with low concentrations of CQDs and Pt salts at pH 4.5, 7.0 and 8.0 were also examined (see Supporting Information Fig. S3). Compared with the original concentration of co-catalyst, both CQDs/K_2PtCl_4 and CQDs/K_2PtCl_6 are sensitive to pH condition and show better performance at pH 7. For the repetitive experiments, unfortunately, the amount of evolved H_2 at the 2nd and 3rd cycle could not reach as much as the amount at the 1st cycle (see Supporting Information Fig. S4).

3.6. Electron transfer from $QuPh^·$–NA to CQDs and Pt salts ($QuPh^·$–NA to CQDs and Pt salt)

Rate constants of electron transfer (k_{obs}) from $QuPh^·$–NA to CQDs or Pt salts in a mixed solution of a KH_2PO_4 buffers (pH 7.0) and MeCN [1:1 (v/v)] were determined by the UV–vis spectral change. This is the first example to determine the electron-transfer rate from a radical species to CQDs directly. An aliquot (2.0 mL) of $QuPh^+$–NA (0.44 mM) was photoirradiated in the presence of NADH (1.0 mM) for several minutes to generate $QuPh^·$–NA. Then, a small portion of an aqueous solution containing CQDs, Pt salts or their mixture was added to the mixed solution containing $QuPh^·$–NA. For CQDs, the UV–vis absorption of $QuPh^·$–NA at 510 nm obviously decrease (see Supporting Information Fig. S5), which indicates electron transfer from $QuPh^·$–NA to CQDs.

The rates of electron transfer (k_{obs}) from $QuPh^·$–NA to CQDs, K_2PtCl_4, K_2PtCl_6 and CQDs/K_2PtCl_6 obeyed first-order kinetics, and

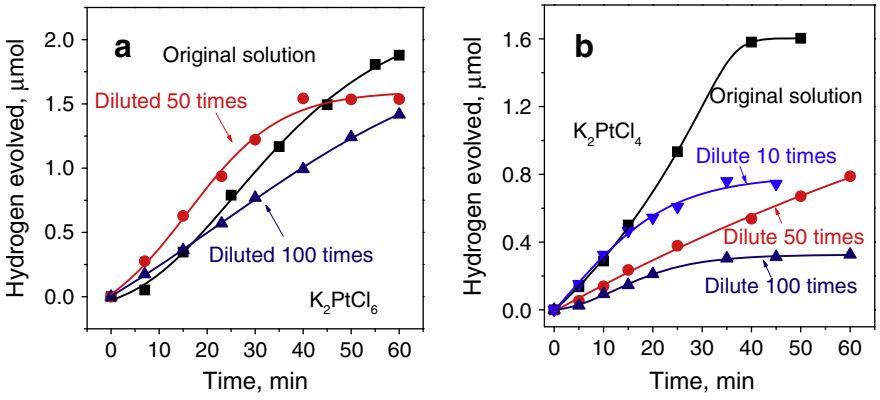

Fig. 6. Time courses of hydrogen evolution under photoirradiation ($\lambda > 340$ nm) of deaerated mixed solutions (2 mL) of KH_2PO_4 buffers (pH = 7.0) and MeCN [1:1 (v/v)] containing $QuPh^+$–NA (0.22 mM), NADH (1.0 mM), with lower concentration of Pt salt and CQDs at 298 K. (a) The original concentration of CQDs and K_2PtCl_6 are 9.4 mg L^{-1} and 7.29 mg L^{-1} respectively, m_{CQDs}:$m_{K2PtCl6}$ = 5:4; (b) the original concentration of CQDs and K_2PtCl_4 are 9.4 mg L^{-1} and 6.23 mg L^{-1} (15 μM) respectively, mCQDs : mK_2PtCl_4 = 3:2.

Please cite this article in press as: W. Wu et al., Photocatalytic H_2 evolution from NADH with carbon quantum dots/Pt and 2-phenyl-4-(1-naphthyl)quinolinium ion, J. Photochem. Photobiol. B: Biol. (2014), http://dx.doi.org/10.1016/j.jphotobiol.2014.10.018

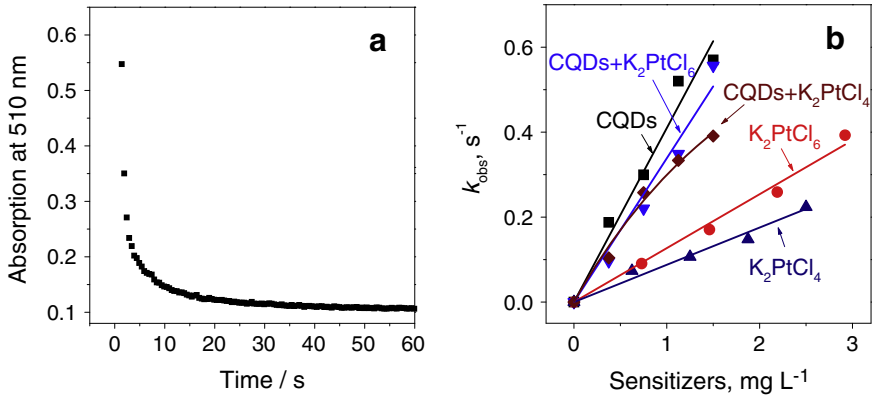

Fig. 7. (a) Decay time profiles of absorption at 510 nm due to QuPh·–NA in the electron transfer from QuPh·–NA to CQDs in a mixed solution (2.0 mL) of a deaerated aqueous buffer (pH 7.0) and MeCN [1:1 (v/v)]. QuPh·–NA was produced by photoirradiation of $QuPh^+$–NA (0.44 mM) in the presence of NADH (1.0 mM). (b) Plots of the pseudo-first-order rate constants (k_{obs}) for electron transfer from $QuPh^+$–NA vs weight concentrations (CQDs, K_2PtCl_6 and K_2PtCl_4).

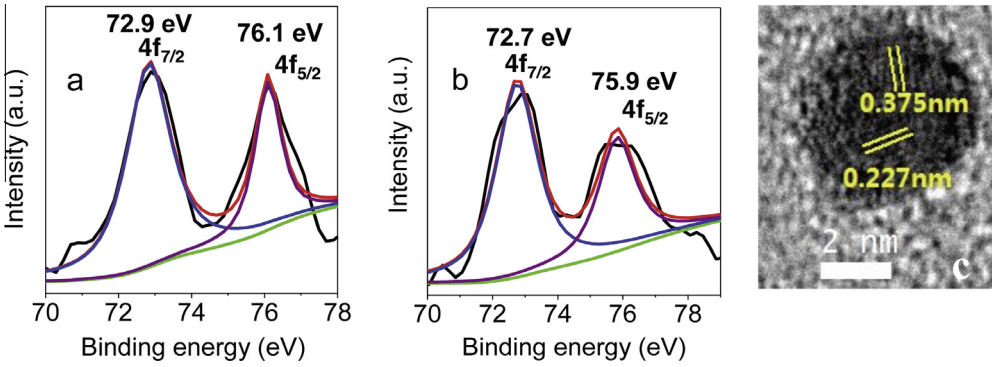

Fig. 8. High-resolution XPS spectrum of Pt 4f from (a) the CQDs/K_2PtCl_6 sample after H_2 evolved reaction; (b) the CQDs/K_2PtCl_4 sample after H_2 evolved reaction; (c) High-resolution TEM (HRTEM) images of CQDs/K_2PtCl_4 sample after H_2 evolved reaction.

the first-order rate constants increased linearly with increasing the amounts of CQDs and Pt salts. The electron-transfer rate constants (k_{et}) were determined from the slopes of the linear plots of k_{obs} versus concentrations of CQDs and Pt salts in Fig. 7. The k_{et} values for CQDs were much larger than K_2PtCl_6 and K_2PtCl_4, indicating that CQDs are a better electron acceptor than K_2PtCl_6 and K_2PtCl_4. In such a case, electron transfer occurs from QuPh·–NA to CQDs firstly, followed by subsequent electron transfer to Pt salts in competition with direct electron transfer from QuPh·–NA to the Pt salts.

TEM images and XPS spectra of the CQDs/Pt after H_2 evolved reaction (Fig. 8) provide valuable information on the catalytically active species. High-resolution XPS spectrum of Pt $4f_{5/2}$ and Pt $4f_{7/2}$ from the CQDs/K_2PtCl_6 sample exhibits binding energies of 76.1 eV and 72.9 eV, respectively (Fig. 8a), which is characteristic of Pt^0 [45], suggesting that electron transfer from QuPh·–NA to CQDs and K_2PtCl_6 results in the reduction of K_2PtCl_6 to Pt^0. Compared with bulk metallic Pt^0 (Pt $4f_{7/2}$, 71.5 eV) [55,56], Pt $4f_{7/2}$ in the CQDs/Pt exhibits a positively shifts of 1.4 eV, suggesting that the electronic environment surrounding the Pt atom is significantly changed due to strong interaction and intimate contact between Pt and graphene carbon. Similar results were also obtained for CQDs/K_2PtCl_4 (Fig. 8b). In order to confirm the existence of Pt^0 in the photocatalytic H_2 evolution reaction, high-resolution TEM (HRTEM) images of CQDs/K_2PtCl_4 sample after the H_2 evolution reaction were measured as shown in Fig. 8c. CQDs/Pt exhibit well-resolved lattice fringes with interplanar spacings of 0.375 nm and 0.227 nm, which are close to the (002) diffraction facets of graphite carbon [49] and the (111) diffraction facets of pure Pt^0 [57], respectively. Compared with the lattice distance of original CQDs before reaction (0.20 nm), the presence of Pt in CQDs results in an increase in the lattice distance due to intimate contact between Pt^0 and CQDs.

4. Conclusions

A highly active and robust catalyst composed of carbon quantum dots and Pt (CQDs/Pt) for H_2 evolution was obtained via an *in situ* facile method with an organic photocatalyst ($QuPh^+$–NA), NADH, CQDs and Pt salts in an aqueous solution under photoirradiation. CQDs/Pt co-catalyst exhibited similar H_2 evolution activity as compared with PtNPs, although the Pt content of CQDs/Pt was only 1/200 of PtNPs. The formation of Pt^0 which has intimate contact with CODs was confirmed by the kinetic, HRTEM and XPS studies. The *in situ* formation of CQDs/Pt reported in this study paves a new way for design of efficient and robust H_2-evolution catalysts.

Acknowledgements

We thank the Grants-in-Aid (Nos. 26620154 and 26288037 to K.O. and Nos. 24350069 and 25600025 to Y.Y.) from the Ministry of Education, Culture, Sports, Science and Technology (MEXT) and an ALCA project from JST, Japan (to S.F.), NSFC (21302224, 51172285), State Key Laboratory of Fine Chemicals (KF1203), China Postdoctoral Science Foundation (2014M560590), Technology Program for Basic Research of Qingdao (14-2-4-47-jch), the

Fundamental Research Funds for the Central Universities (13CX02066A, 14CX02060A) and Shandong Provincial Natural Science Foundation (ZR2013BQ028) for financial support.

Appendix A. Supplementary material

Supplementary data associated with this article can be found, in the online version, at http://dx.doi.org/10.1016/j.jphotobiol.2014.10.018.

References

[1] L. Chen, M. Wang, K. Han, P. Zhang, F. Gloaguen, L. Sun, A super-efficient cobalt catalyst for electrochemical hydrogen production from neutral water with 80 mV over potential, Energy Environ. Sci. 7 (2014) 329–334.
[2] Z.-J. Li, J.-J. Wang, X.-B. Li, X.-B. Fan, Q.-Y. Meng, K. Feng, B. Chen, C.-H. Tung, L.-Z. Wu, An exceptional artificial photocatalyst, Ni_h-CdSe/CdS core/shell hybrid, made in situ from cdse quantum dots and nickel salts for efficient hydrogen evolution, Adv. Mater. 25 (2013) 6613–6618.
[3] F. Wang, W.-G. Wang, X.-J. Wang, H.-Y. Wang, C.-H. Tung, L.-Z. Wu, A highly efficient photocatalytic system for hydrogen production by a robust hydrogenase mimic in an aqueous solution, Angew. Chem. Int. Ed. 50 (2011) 3193–3197.
[4] S. Dunn, Hydrogen History of Encyclopedia of Energy, vol. 3, Elsevier, New York, 2004.
[5] M. Momirlan, T.N. Veziroglu, The properties of hydrogen as fuel tomorrow in sustainable energy system for a cleaner planet, Int. J. Hydrogen Energy 30 (2005) 795–802.
[6] J.A. Turner, Sustainable hydrogen production, Science 305 (2004) 972–974.
(7) R.A. Kerr, R.F. Service, What can replace cheap oil—and when?, Science 309 (2005) 101
[8] S. Fukuzumi, Bioinspired energy conversion systems for hydrogen production and storage, Eur. J. Inorg. Chem. (2008) 1351–1362.
[9] S. Fukuzumi, Y. Yamada, T. Suenobu, K. Ohkubo, H. Kotani, Catalytic mechanisms of hydrogen evolution with homogeneous and heterogeneous catalysts, Energy Environ. Sci. 4 (2011) 2754–2766.
[10] S. Fukuzumi, Y. Yamada, Catalytic activity of metal-based nanoparticles for photocatalytic water oxidation and reduction, J. Mater. Chem. A 22 (2012) 24284–24296.
[11] T.A. Faunce, W. Lubitz, A.W. Rutherford, D. MacFarlane, G.F. Moore, P. Yang, D.G. Nocera, T.A. Moore, D.H. Gregory, S. Fukuzumi, K.B. Yoon, F.A. Armstrong, M.R. Wasielewski, S. Styring, Energy and environment policy case for a global project on artificial photosynthesis, Energy Environ. Sci. 6 (2013) 695–698.
[12] Y. Tachibana, L. Vayssieres, J.R. Durrant, Artificial photosynthesis for solar water-splitting, Nat. Photon. 6 (6) (2012) 511–518.
[13] P.V. Kamat, Meeting the clean energy demand: nanostructure architectures for solar energy conversion, J. Phys. Chem. C 111 (2007) 2834–2860.
[14] A.J. Bard, M.A. Fox, Artificial photosynthesis: solar splitting of water to hydrogen and oxygen, Acc. Chem. Res. 28 (1995) 141–145.
[15] Y. Yamada, T. Kotani, H. Miyahigashi, K. Ohkubo, S. Fukuzumi, Photocatalytic hydrogen evolution under highly basic conditions by using Ru nanoparticles and 2-phenyl-4-(1-naphthyl)quinolinium ion, J. Am. Chem. Soc. 133 (2011) 16136–16145.
[16] H. Kotani, R. Hanazaki, K. Ohkubo, Y. Yamada, S. Fukuzumi, Size-and shape-dependent activity of metal nanoparticles as hydrogen-evolution catalysts: mechanistic insights into photocatalytic hydrogen evolution, Chem. Eur. J. 17 (2011) 2777–2785.
[17] H. Kotani, K. Ohkubo, Y. Takai, S. Fukuzumi, Viologen-modified platinum clusters acting as an efficient catalyst in photocatalytic hydrogen evolution, J. Phys. Chem. B 110 (2006) 24047–24053.
[18] M.M. Najafpour, S. Heidari, E. Amini, M. Khatamian, R. Carpentier, S.I. Allakhverdiev, Nano-sized layered Mn oxides as promising and biomimetic water oxidizing catalysts for water splitting in artificial photosynthetic systems, J. Photochem. Photobiol. B Biol. 133 (2014) 124–139.
[19] S.I. Allakhverdiev, Recent progress in the studies of structure and function of photosystem II, J. Photochem. Photobiol. B Biol. 104 (2011) 1–8.
[20] S. Haripriya, M.V. Sangaranarayanan, Influence of the work function on electron transfer processes at metals: application to the hydrogen evolution reaction, Langmuir 18 (2002) 5572–5578.
[21] T.S. Ahmadi, Z.L. Wang, T.C. Green, A. Henglein, M.A. El-Sayed, Shape-controlled synthesis of colloidal platinum nanopaticles, Science 272 (1996) 1924–1926.
[22] J.N. Kuhn, W. Huang, C.-K. Tsung, Y. Zhang, G.A. Somorjai, Structure sensitivity of carbon-nitrogen ring opening: impact of platinum particle size from below 1 to 5 nm upon pyrrole hydrogenation product selectivity over monodisperse platinum nanoparticles loaded onto mesoporous silica, J. Am. Chem. Soc. 130 (2008) 14026–14027.
[23] C.-K. Tsung, J.N. Kuhn, W. Huang, C. Aliaga, L.-I. Hung, G.A. Somorjai, P. Yang, Sub-10 nm platinum nanocrystals with size and shape control: catalytic study for ethylene and pyrrole hydrogenation, J. Am. Chem. Soc. 131 (2009) 5816–5822.
[24] H. Lee, S.E. Habas, S. Kweskin, D. Butcher, G.A. Somorjai, P. Yang, Morphological control of catalytically active platinum nanocrystals, Angew. Chem. Int. Ed. 118 (2006) 7988–7992.
[25] H. Lee, S.E. Habas, S. Kweskin, D. Butcher, G.A. Somorjai, P. Yang, Morphological control of catalytically active platinum nanocrystals, Angew. Chem. Int. Ed. 45 (2006) 7824–7828.
[26] H. Song, F. Kim, S. Connor, G.A. Somorjai, P. Yang, Pt nanocrystals: shape control and langmuir–blodgett monolayer formation, J. Phys. Chem. B 109 (2005) 188–193.
[27] Y. Sun, Z. Lin, J. Lu, X. Hong, P. Liu, Collapse in crystalline structure and decline in catalytic activity of Pt nanoparticles on reducing particle size to 1 nm, J. Am. Chem. Soc. 129 (2007) 15465–15467.
[28] E. Schmidt, A. Vargas, T. Mallat, A. Baiker, Shape-selective enantioselective hydrogenation on pt nanoparticles, J. Am. Chem. Soc. 131 (2009) 12358–12367.
[29] R. Narayanan, M.A. El-Sayed, Shape-dependent catalytic activity of platinum nanoparticles in colloidal solution, Nano Lett. 4 (2004) 1343–1348.
[30] S. Park, Y. Xie, M.J. Weaver, Electrocatalytic pathways on carbon-supported platinum nanoparticles: comparison of particle-size-dependent rates of methanol, formic acid, and formaldehyde electrooxidation, Langmuir 18 (2002) 5792–5798.
[31] M. Arenz, K.J.J. Mayrhofer, V. Stamenkovic, B.B. Blizanac, T. Tada, P.N. Ross, N.M. Markovic, The effect of the particle size on the kinetics of CO electrooxidation on high surface area Pt catalysts, J. Am. Chem. Soc. 127 (2005) 6819–6829.
[32] M. Grätzel, Artificial photosynthesis: water cleavage into hydrogen and oxygen by visible light, Acc. Chem. Res. 14 (1981) 376–384.
[33] N. Toshima, M. Kuriyama, Y. Yamada, H. Hirai, Colloidal platinum catalyst for light-induced hydrogen evolution from water: a particle size effect, Chem. Lett. (1981) 793–796.
[34] N. Toshima, K. Hirakawa, Polymer-protected bimetallic nanocluster catalysts having core/shell structure for accelerated electron transfer in visible-light-induced hydrogen generation, Polymer J. 31 (1999) 1127–1132.
[35] N. Toshima, Core/shell-structured bimetallic nanocluster catalysts for visible-light-induced electron transfer, Pure Appl. Chem. 72 (2000) 317–325.
[36] G. Schmid, Large clusters and colloids. metals in the embryonic state, Chem. Rev. 92 (1992) 1709–1727.
[37] N. Toshima, T. Yonezawa, Bimetallic nanoparticles-novel materials for chemical and physical applications, New J. Chem. 22 (1998) 1179–1201.
[38] N.T. Nguyen, J. Yoo, M. Altomare, P. Schmuki, "Suspended" Pt nanoparticles over TiO_2 nanotubes for enhanced photocatalytic H_2 evolution, Chem. Commun. 50 (2014) 9653–9656.
[39] T. Hasobe, H. Sakai, K. Mase, K. Ohkubo, S. Fukuzumi, Remarkable enhancement of photocatalytic hydrogen evolution efficiency utilizing an internal cavity of supramolecular porphyrin hexagonal nanocylinders under visible-light irradiation, J. Phys. Chem. C 117 (2013) 4441–4449.
[40] Y. Yamada, H. Tadokoro, S. Fukuzumi, Hybrid H_2-evolution catalysts: in situ formation of H_2-evolution catalysts from metal salts inside the mesopores of silica–alumina supporting an organic photosensitiser, RSC Adv. 3 (2013) 25677–25680.
[41] H. Li, X. He, Z. Kang, H. Huang, Y. Liu, J. Liu, S. Lian, C.H.A. Tsang, X. Yang, S.-T. Lee, Water-soluble fluorescent carbon quantum dots and photocatalyst design, Angew. Chem. Int. Ed. 49 (2010) 4430–4434.
[42] D. Tang, H. Zhang, H. Huang, R. Liu, Y. Han, Y. Liu, C. Tong, Z. Kang, Carbon quantum dots enhance the photocatalytic performance of $BiVO_4$ with different exposed facets, Dalton Trans. 42 (2013) 6285–6289.
[43] X. Zhang, F. Wang, H. Huang, H. Li, X. Han, Y. Liu, Z. Kang, Carbon quantum dot sensitized TiO_2 nanotube arrays for photoelectrochemical hydrogen generation under visible light, Nanoscale 5 (2013) 2274–2278.
[44] H. Li, Z. Kang, Y. Liu, S.-T. Lee, Carbon nanodots: synthesis, properties and applications, J. Mater. Chem. 22 (2012) 24230–24253.
[45] Q. Li, C. Cui, H. Meng, J. Yu, Visible-light photocatalytic hydrogen production activity of $ZnIn_2S_4$ microspheres using carbon quantum dots and platinum as dual co-catalysts, Chem. Asian J. 9 (2014) 1766–1770.
[46] X. Zhang, H. Huang, J. Liu, Y. Liu, Z. Kang, Carbon quantum dots serving as spectral converters through broadband upconversion of near-infrared photons for photoelectrochemical hydrogen generation, J. Mater. Chem. A 1 (2013) 11529–11533.
[47] H. Yu, Y. Zhao, C. Zhou, L. Shang, Y. Peng, Y. Cao, L.Z. Wu, C.-H. Tung, T. Zhang, Carbon quantum dots/TiO_2 composites for efficient photocatalytic hydrogen evolution, J. Mater. Chem. A 2 (2014) 3344–3351.
[48] H. Kotani, K. Ohkubo, S. Fukuzumi, Formation of a long-lived electron-transfer state of a naphthalene–quinolinium ion dyad and the π-dimer radical cation, Faraday Discuss. 155 (2012) 89–102.
[49] H. Nie, M. Li, Q. Li, S. Liang, Y. Tan, L. Sheng, W. Shi, S.X.-A. Zhang, Carbon dots with continuously tunable full-color emission and their application in ratiometric pH sensing, Chem. Mater. 26 (2014) 3104–3112.
[50] S. Hu, R. Tian, L. Wu, Q. Zhao, J. Yang, J. Liu, S. Cao, Chemical regulation of carbon quantum dots from synthesis to photocatalytic activity, Chem. Asian J. 8 (2013) 1035–1041.
[51] Y. Liu, Y.-X. Yu, W.-D. Zhang, Carbon quantum dots-doped CdS microspheres with enhanced photocatalytic performance, J. Alloy. Compd. 569 (2013) 102–110.
[52] Y. Deng, D. Zhao, X. Chen, F. Wang, H. Song, D. Shen, Long lifetime pure organic phosphorescence based on water soluble carbon dots, Chem. Commun. 49 (2013) 5751–5753.

Please cite this article in press as: W. Wu et al., Photocatalytic H_2 evolution from NADH with carbon quantum dots/Pt and 2-phenyl-4-(1-naphthyl)quinolinium ion, J. Photochem. Photobiol. B: Biol. (2014), http://dx.doi.org/10.1016/j.jphotobiol.2014.10.018

[53] L. Al-Mashat, K. Shin, K. Kalantar-zadeh, J.D. Plessis, S.H. Han, R.W. Kojima, R.B. Kaner, D. Li, X. Gou, S.J. Ippolito, W. Wlodarski, Graphene/polyaniline nanocomposite for hydrogen sensing, J. Phys. Chem. C 114 (2010) 16168–16173.

[54] Y. Yamada, S. Shikano, S. Fukuzumi, Robustness of Ru/SiO_2 as a hydrogen-evolution catalyst in a photocatalytic system using an organic photocatalyst, J. Phys. Chem. C 117 (2013) 13143–13152.

[55] C. Petit, M. Seredych, T.J. Bandosz, Revisiting the chemistry of graphite oxides and its effect on ammonia adsorption, J. Mater. Chem. 19 (2009) 9176–9185.

[56] D. Chen, Y. Zhao, Y. Fan, X. Peng, X. Wang, J. Tian, Synthesis of Ni@PbPt supported on graphene by galvanic displacement reaction for improving ethanol electro-oxidation, J. Mater. Chem. A 1 (2013) 13227–13232.

[57] W.-H. Yang, H.-H. Wang, D.-H. Chen, Z.-Y. Zhou, S.-G. Sun, Facile synthesis of a platinum–lead oxide nanocomposite catalyst with high activity and durability for ethanol electrooxidation, Phys. Chem. Chem. Phys. 14 (2012) 16424–16432.

Please cite this article in press as: W. Wu et al., Photocatalytic H_2 evolution from NADH with carbon quantum dots/Pt and 2-phenyl-4-(1-naphthyl)quinolinium ion, J. Photochem. Photobiol. B: Biol. (2014), http://dx.doi.org/10.1016/j.jphotobiol.2014.10.018